MULTI-BUNCH INSTABILITIES MEASUREMENT AND ANALYSIS AT THE DIAMOND LIGHT SOURCE

R. Bartolini[1], R. Fielder, E. Koukovini-Platia, G. Rehm, Diamond Light Source, Oxfordshire, UK
[1]also at John Adams Institute, University of Oxford, UK

Abstract

The characterisation of the multi-bunch dynamics at the Diamond Light Source is performed with a very advanced transverse multi-bunch feedback (TMBF) system that operates fast grow damp experiments thus allowing the exploration of many machine conditions. We report here the latest results of the measurement campaign, the implication on the machine impedance model and some of the intricacies of the analysis and interpretation of the experimental data.

INTRODUCTION

Multibunch collective effects can be one of the limiting factors for increasing current and reducing vacuum chamber size in synchrotron light sources. They are driven by long-range wakefields generated primarily by resonant structures formed by the vacuum chamber, and the resistive wall (RW) impedance due to the finite conductivity of the chamber material. Fast ion instabilities form a third source of multibunch instabilities, but are usually only present during conditioning of newly installed components and do not pose a problem for normal operation.

As light sources such as Diamond Light Source (DLS) push for lower emittance, RW impedance can become more significant due to the narrower vacuum chambers used to allow higher magnetic fields. This also has the effect of bringing resonant structures such as flanges and beam position monitors (BPMs) closer to the electron beam, potentially increasing the impedance from these sources as well. A campaign of measurements and simulations is ongoing to characterise the impedance of the DLS storage ring.

THEORY

For M bunches with finite length, internal modes and non-zero chromaticity the complex frequency shift of the mode (μ, l) is given by [1]:

$$\Omega^{(\mu,l)} - \omega_\beta = -i\frac{MNr_0c}{2\gamma T_0^2\omega_\beta}\sum_{p=-\infty}^{\infty} Z_1^\perp(\omega_{\mu,l})\cdot h_l\left(\omega_{\mu,l}-\omega_\xi\right)$$

where ω_β is the unperturbed betatron frequency, N is the number of particles per bunch, r_0 is the classical radius of the particle, γ is the Lorentz factor, T_0 is the revolution period, $Z_l^\perp$ is the transverse dipole impedance and h_l is the bunch mode spectral power. Mode (μ, l) is driven by the impedance sampled at the discrete set of frequencies:

$$\omega_{\mu,l} = (pM+\mu)\omega_0 + \omega_\beta + l\omega_s$$

where ω_s is the synchrotron frequency.

The coherent frequency shift and growth rate are $\mathrm{Re}\Omega^{(\mu,l)} - \omega_\beta$ and $\mathrm{Im}\Omega^{(\mu,l)}$, respectively. A mode μ sampled bunch-by-bunch corresponds to the frequency $\mu\omega_0 + \Omega_{x,y}$ aliased in $[0, M\omega_0]$, the baseband of the RF. For a real signal the spectrum is further folded symmetrically in $[0, M\omega_0/2]$.

Growth Rate Fitting

$Z_l^\perp$ is given by the sum of all transverse impedances present. The impedance of the Diamond ring is considered to consist primarily of resistive wall plus some number of narrowband resonators, i.e.

$$Z_\perp = Z_\perp^{RW} + \sum Z_\perp^{res}$$

$Z_\perp^{RW}$ is given by [1]:

$$\frac{Z_{x,y}^{rw}}{L} = G_{1x,y}\frac{\mathrm{sgn}(\omega)+i}{\pi b^3}\sqrt{\frac{Z_0 c\rho}{2}}|\omega|^{-1/2} \quad (1)$$

where b is the half-aperture of the vacuum chamber, $G_{1x,y}$ is the form factor of the elliptical chamber, Z_0 is the free space impedance, c is the speed of light, and ρ is the resistivity. For Diamond, the chamber was treated as only stainless steel with resistivity of $6.90*10^{-7}$ Ωm.

$Z_\perp^{res}$ is given by:

$$Z_\perp^{res} = \frac{R_S}{\frac{\omega}{\omega_r}+iQ\left(\frac{\omega^2}{\omega_r^2}-1\right)} \quad (2)$$

where R_s is the shunt impedance, Q is the quality factor and ω_r is the characteristic frequency of the resonator.

MEASUREMENTS

Grow-damp measurements are carried out by exciting mode μ for some number of turns, typically around 250, using a stripline driven at a frequency (pM + μ)ω0 + ωβ, then stopping the excitation and measuring the free oscillations, which may be naturally damped or anti-damped. The TMBF [2] is then run as feedback to damp any residual oscillations. This is repeated for all modes, or for any subset desired. The damping time or growth rate of each mode can be found from a linear fit on the log of the amplitude, as shown in Fig. 1.

This method places some clear restrictions on the possible conditions, since if a mode is naturally unstable the beam can blow up and be lost during the measurement. At zero vertical chromaticity, we find a limit of about 20 mA total beam current. At higher chromaticities measurements are possible up to the maximum of 300 mA.

In addition, the hardware buffer for the TMBF system can only hold data for ~2.5 million turns, meaning the measurements are limited to 2500 turns per mode. Typically this will be composed of 250 turns forced excitation, 1750 turns free oscillation and 500 turns active damping, but more damping time may be required under some operating conditions.

ISBN 978-3-95450-182-3

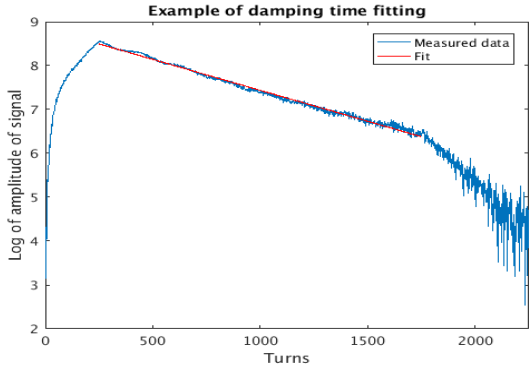

Figure 1: Example of grow-damp measurement of a single stable mode on semi-log scale with linear fit to damping time.

RESULTS

Diamond Storage Ring

The Diamond storage ring has a harmonic number h = 936, with a 533 kHz revolution frequency, giving a 2 ns (500 MHz) repetition rate. Total beam current is up to 300 mA, with a bunch length of 15-25 ps; results shown here were taken at 200 mA unless otherwise stated. In the current optics since installation of the double-double bend achromat (DDBA) section [4], tunes are $Q_x = 0.172$ and $Q_y = 0.273$, while average beta functions were taken to be $\beta_x = 10.24$ m and $\beta_y = 13.16$ m. Chamber aperture, b, was treated as the fitting parameter for the resistive wall impedance. The contribution of radiation and chromatic damping was removed from measurements except where that was the property of interest.

Bare Lattice

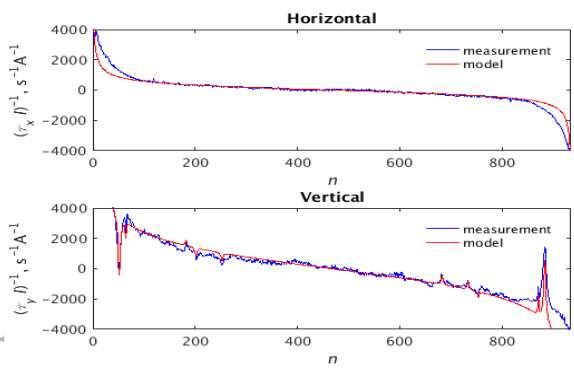

Figure 2: Measured damping rates for all modes and fit with resistive wall and resonators.

With all in-vacuum insertion devices (IDs) open, the damping rates in horizontal and vertical planes are as shown in Fig. 2. The horizontal is observed to be dominated by resistive wall with no significant resonators or other impedance sources (top). The vertical has five peaks corresponding to resonators in addition to the RW impedance (bottom). The largest of these, centred on mode 53, has been identified as caused by the vertical collimator (see below). A high-Q resonance at mode 82 has yet to be identified. The other three, clustered around mode 200, appear to correspond to various ID straights. The best fit for the resistive wall impedances were with b = 14.0 mm in the horizontal and 10.3 mm in the vertical.

Vertical Collimator

The vertical collimator had previously been identified as the cause of the largest measured peak in impedance [3]. During commissioning of the DDBA section [4,5], the collimator was found by beam-based aperture measurements to be 0.9 mm off-centre. This offset was corrected, and a new setting for the gap (2.4 mm half-aperture) was found to ensure the narrower vessel in DDBA was protected from beam losses. This resulted in the peak moving from mode 22 to mode 53, with a symmetric peak at mode 884. This peak was fitted by a resonator with parameters $R_s = 3$ MΩ/m, $Q = 500$, $f = \omega/2\pi = 1.47$ GHz. The behaviour of the peak as the collimator is moved remains similar to that previously measured despite the removal of a significant asymmetry [3].

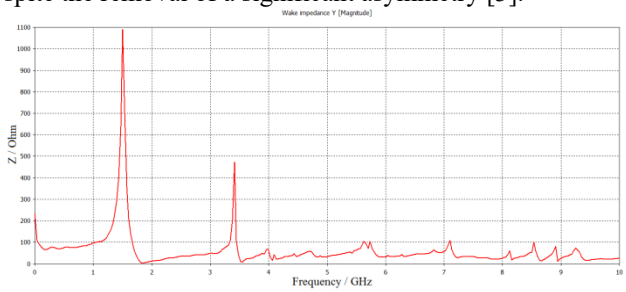

Figure 3: Vertical impedance from CST [6] simulation of vertical collimator.

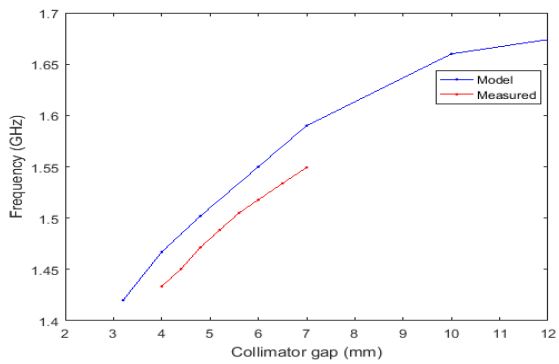

Figure 4. Change in frequency of main impedance peak vs. vertical collimator gap from CST (blue) and measurements (red).

Simulations of the vertical collimator in CST Studio show a large peak in impedance at 1.50 GHz for a 2.4 mm half-gap, matching closely with the fitted value (Fig. 3). The frequency of this peak varies in the same way as the measured peak corresponding to mode 884 (Fig. 4), although with some small offset between model and measurement.

Insertion Devices

The effect of closing in-vacuum insertion devices, both all together and individually, has been measured. Since IDs only move in the vertical plane, no effect on the horizontal impedance is present. The IDs create three peaks in

the vertical impedance, one high-Q at mode 160, and two broader peaks centred around modes 120 and 190 (Fig. 5). However, these broader peaks are composed of multiple sharper peaks rather than being single low-Q resonators.

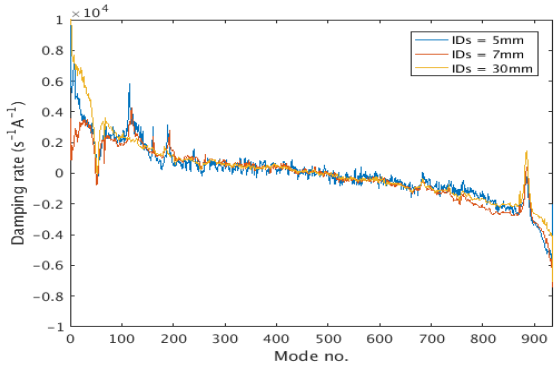

Figure 5: Vertical damping rates for all modes vs. in-vacuum ID gap at 30 mm (fully open), 7 mm (gap used during injection) and 5 mm (minimum gap).

Since the transverse impedance is antisymmetric in the frequency domain, it is expected that the effect of impedance is reflected in a similar asymmetry in the multi-bunch mode spectrum, with an unstable mode n corresponding to an equally stable mode h-n, where h=936 for Diamond. This can be observed here with, for example, the large peak caused by the vertical collimator. However, the effects of the IDs do not show this behaviour, with significant peaks in impedance at low modes not reflected in the corresponding high modes (Fig. 6). This behaviour is as yet unexplained and is under investigation.

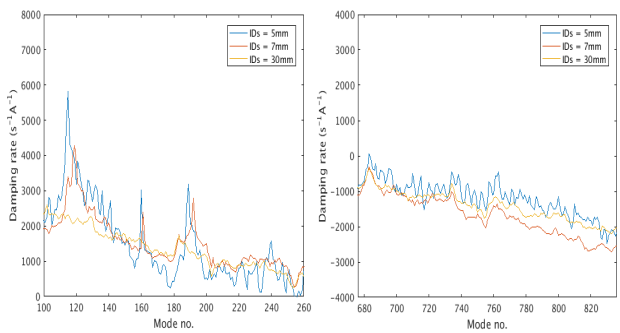

Figure 6. Detail of effect of IDs in modes 100-260 (left) and symmetric region in modes 676-836 (right).

It has further been seen that there is a qualitative difference between IDs installed at different times in Diamond. Phase 1 [7] IDs primarily contribute only to the peaks around mode 120, while phase 2 IDs contribute to both those around modes 120 and modes 190. The sole cryogenic permanent magnet undulator (CPMU) currently installed is also observed to behave somewhat differently from the others, although its effects still appear around the same frequencies. Simulations in CST Studio suggest these differences are largely due to the different designs of transitional tapers leading from the beam pipe to the ID vessels. Since simulating such large structures in the required detail presents something of a challenge, some effort has been made to measure the resonances within the ID vessel by other means [8].

RF Voltage

Although RF voltage has no direct effect on impedance or transverse damping rates, changes in bunch length will alter the bunch spectrum and therefore affect how the impedance spectrum is sampled. Figure 7 shows that there is no measurable trend in damping rates with RF voltage in either plane. However, it is clear that the beam becomes increasingly unstable when the voltage is below 2.4 MV.

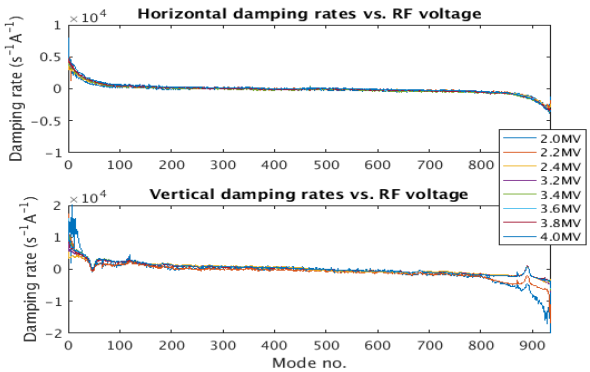

Figure 7: Vertical damping rates for all modes vs. RF voltage.

DDBA Upgrade

The change in impedance due to installation of the DDBA section was measured and fitted [9]. Figure 8 shows the difference in damping rates before and after DDBA installation with all IDs closed to minimum gaps. Aside from the movement of the vertical collimator, the only significant change observed is an increase in resistive wall impedance; no new peaks are seen.

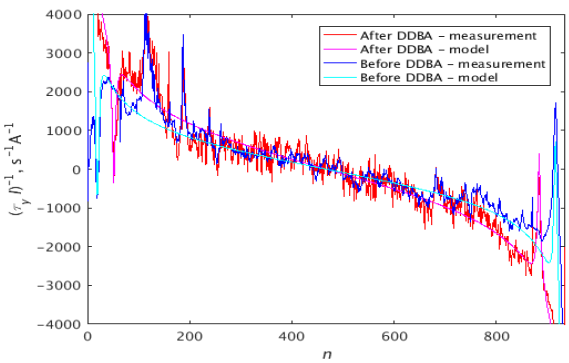

Figure 8. Vertical damping rates before (blue) and after (red) installation of DDBA section.

CONCLUSIONS

A comprehensive program of measurements of instabilities and impedance is ongoing at Diamond, in combination with simulations and comparisons with theory to identify and analyse the sources of these impedances.

REFERENCES

[1] A. W. Chao. *Physics of Collective Beam Instabilities in High Energy Accelerators*. New York, USA: Wiley, 1993.

ISBN 978-3-95450-182-3

[2] G. Rehm, M.G. Abbott, A.F.D. Morgan, in *Proc. IBIC'14,* pp. 696-699.

[3] R. Bartolini, R. Fielder, G. Rehm, in *Proc. IPAC'16*, pp. 1685-1687.

[4] R. Bartolini, *et al.*, "The DDBA cell upgrade at Diamond: from design to commissioning", presented at IPAC'17, Copenhagen, Denmark, May 2017, paper WEPAB092, this conference.

[5] I. Martin, *et al.*, "Electron beam commissioning of the DDBA modification to the Diamond storage ring", presented at IPAC'17, Copenhagen, Denmark, May 2017, paper WEPAB095, this conference.

[6] CST Studio Suite, `https://www.cst.com`

[7] Z. Patel, *et al.*, "Insertion devices at Diamond Light Source: a retrospective plus future developments", presented at IPAC'17, Copenhagen, Denmark, May 2017, paper TUPAB116, this conference.

[8] G. Rehm, "Measurement of RF resonances and measured impact on transverse multibunch instabilities from in-vacuum insertion devices", presented at IPAC'17, Copenhagen, Denmark, May 2017, paper WEPIK102, this conference.

[9] E. Koukovini-Platia, L.M. Bobb, R. Fielder, R. Bartolini, "Collective effects studies of the double-double bend achromat cell at Diamond", presented at IPAC'17, Copenhagen, Denmark, May 2017, paper THPVA030, this conference.